Ultrasound-triggered sonocatalytic reduction of CO_2 via $H_2Ti_3O_7$ nanowires ⊘

Jiangping Ma; Xin Xiong; Chaogang Ban; Kaiwen Wang ⓘ ; Ji-Yan Dai ✉ ⓘ ; Xiaoyuan Zhou ✉ ⓘ

Check for updates

View Online

Export Citation

Articles You May Be Interested In

TiO_2-supported Au_{144} nanoclusters for enhanced sonocatalytic performance

J. Chem. Phys. (September 2021)

Effect of CeO_2 promotion on the sonocatalytic performance of ZrO_2 nanoparticle catalysts

AIP Conf. Proc. (October 2018)

From nanotubes to single crystals: Co doped TiO_2

APL Mater. (September 2013)

Ultrasound-triggered sonocatalytic reduction of CO_2 via $H_2Ti_3O_7$ nanowires

Jiangping Ma,[1] Xin Xiong,[1] Chaogang Ban,[1] Kaiwen Wang,[2] Ji-Yan Dai,[3,a] and Xiaoyuan Zhou[1,4,a]

AFFILIATIONS

[1]College of Physics and Center of Quantum Materials and Devices, Chongqing University, Chongqing 401331, China
[2]Beijing Key Lab of Microstructure and Properties of Advanced Materials, Beijing University of Technology, Beijing 100124, China
[3]Department of Applied Physics, The Hong Kong Polytechnic University, Hong Kong 999077, China
[4]State Key Laboratory of Coal Mine Disaster Dynamics and Control, Chongqing University, Chongqing 401331, China

[a]Authors to whom correspondence should be addressed: jiyan.dai@polyu.edu.hk and xiaoyuan2013@cqu.edu.cn

ABSTRACT

Ultrasound-stimulated piezo-electrocatalysis has been studied for a period; however, the mechanism is still unclear mainly due to the coexistence with other multiple effects like sonocatalysis, which was usually ignored. In this work, with the non-piezoelectric $H_2Ti_3O_7$ nanowires following the same experimental process in piezo-electrocatalysis, the sonocatalytic reduction performance of CO_2 is investigated. By applying vibration under the excitation of ultrasound with various frequencies and powers, it is found that CO is the ultimate product with a selectivity of 100%, and the optimal CO yield of 8.3 μmol g^{-1} h^{-1} is achieved with the addition of sacrificial agents. The $H_2Ti_3O_7$ catalysts are also found to present a good recycling utilization ability. This work indicates that the sonocatalysis effect may exist in the piezo-electrocatalytic process using the ultrasonic excitation, which is suggested to be taken into consideration when exploring the mechanism of piezo-electrocatalysis in the future.

Published under an exclusive license by AIP Publishing. https://doi.org/10.1063/5.0130990

Converting the excessive CO_2 emission into value-added fuels has been attracting great interest due to its potential of mitigating fossil combustion and abating carbon emissions.[1] Over the past decades, scientists have made enormous efforts to explore techniques to harvest various renewable energies, such as electricity-driven electrocatalysis,[2] light-driven photocatalysis,[3] and heat-driven thermocatalysis.[4] These techniques have attracted unprecedented research enthusiasm and demonstrated great potential in terms of dealing with the environmental crisis and the growing demand for clean energies. In addition to the above-mentioned renewable energy sources, utilization of dispersed and extensive mechanical energy in catalysis draws relatively little attention.

The piezoelectric effect, discovered by the Curie brothers in 1880,[5] demonstrates the electricity generation ability of piezoelectric materials when subjected to mechanical vibration and vice versa. Based on this electromechanical property, piezoelectric materials were used to be extensively exploited as the ignition source for cigarette lighters,[6] nanogenerators,[7] sensors,[8] inkjet printing,[9] and ultrasonic imaging.[10] In 2010, Hong et al. expanded the piezoelectricity to electrochemical functionality and proposed a piezoelectrochemical system (i.e., piezo-electrocatalysis) for hydrogen generation from pure water by using ultrasound as a mechanical excitation source.[11] Afterward, many piezo-electrocatalytic applications were developed, including degradation of pollutants,[12,13] organic synthesis,[14] tooth whitening,[15] tumor therapy,[16] and generation of reactive oxygen species.[17] Recently, we reported the piezo-electrocatalysis for a CO_2 reduction technique, opening an avenue for CO_2 utilization by harvesting the mechanical vibration energy.[18] Several high-quality reviews have systematically summarized and discussed the advanced procedures from the perspective of material design and applications.[19] However, the mechanism of piezo-electrocatalysis is still unclear,[20] which can largely be ascribed to its coexistence with multiple other effects, e.g., the sonocatalysis effect. Sonocatalysis may cause an effect on the catalytic performance.

Sonocatalysis is activated by the ultrasonic cavitation-induced sonoluminescence effect,[21] in which the electron–hole pairs can be separated to conduction band (CB) and valence band (VB), respectively. Being similar to the mechanism of photocatalytic semiconductors, these electrons/holes on the proper CB/VB positions can initiate the reactions. Actually, piezo-electrocatalysis and sonocatalysis have the same experimental process. To specify, the catalysts are added into the solution with some reactants or bubbled with reaction gases, which is sealed in a reactor and subsequently subjected to the ultrasonic excitation to

detect the ultimate products. The difference between the two catalytic techniques lies in their crystal structures. Piezo-electrocatalysis demands that the materials must be non-centrosymmetric, while sonocatalysis seems to be independent of the non-centrosymmetric crystal structure but related to proper band positions. In addition, piezoelectric materials are generally insulators, implying that they possess appropriate band structures and can exhibit the sonocatalysis effect themselves. Taking the typical piezoelectric $BaTiO_3$ as an example, it has a bandgap of $\sim$3.3 eV, CB potential of $\sim$$-1.3$ eV, and VB potential of $\sim$2 eV vs the normal hydrogen electrode (NHE).[22] The CB potential of $BaTiO_3$ satisfies the redox potential -0.53 eV of CO_2-to-CO and -0.41 eV of H_2O-to-H_2, implying that $BaTiO_3$ can potentially achieve these reactions via the sonocatalysis effect. However, the sonocatalysis effect is usually ignored in the investigation of piezo-electrocatalysis.

In this work, the centrosymmetric $H_2Ti_3O_7$ nanowire, as the precursor of synthesizing barium titanate, is found to present the sonocatalysis effect in CO_2 reduction. Under the conditions of applying ultrasound energy and sacrificial agents, the non-piezoelectric $H_2Ti_3O_7$ can convert CO_2 into CO with a maximum yield of 8.3 μmol g^{-1} h^{-1}. Our work indicates that the sonocatalysis effect may exist in the piezo-electrocatalytic process under the ultrasonic excitation, which is suggested to be taken into consideration when exploring its mechanism in the future.

Structural and morphological characterization results of the $H_2Ti_3O_7$ nanowires are shown in Fig. 1. X-ray diffraction (XRD) pattern is used to determine the structure phase of the $H_2Ti_3O_7$ nanowires as shown in Fig. 1(a), where the observed strong diffraction peaks at $2\theta = 10.9°$, 25.0°, and 48.7° can be indexed as the (200), (202), and (114) planes of monoclinic $H_2Ti_3O_7$ (JCPDS 47-0561, space group $C2/m$).[23] The XRD pattern presents only the characteristic peaks of $H_2Ti_3O_7$ without other phase, suggesting the preparation of the $H_2Ti_3O_7$ catalysts. Figure 1(b) shows scanning electron microscopy (SEM) image of the $H_2Ti_3O_7$ nanowires, from which their average length of $>$10 μm can be determined. The nanowire morphology is also shown by low-magnification transmission electron microscopy (TEM) image in Fig. 1(c), and more detailed crystal structure of the nanowires is revealed by high-resolution TEM characterization as presented in Fig. 1(d). It is apparent that the $H_2Ti_3O_7$ nanowires are the single crystalline structure with lattice distances of 0.215 and 0.338 nm [Fig. 1(e)] corresponding to the d-spacing of (204) and (111) planes, respectively. Figure 1(f) shows the selected-area electron diffraction (SAED) pattern of the $H_2Ti_3O_7$ catalysts which further proves its crystal structure. In addition, elemental mapping measured by energy dispersive x-ray spectroscopy in Fig. 1(g) indicates that Ti and O are uniformly distributed throughout the nanowires.

X-ray photoelectron spectroscopy (XPS) analysis was performed to further investigate the element composition and chemical states of the as-synthesized $H_2Ti_3O_7$ catalysts. Clear Ti 2p and O 1s peaks can be seen in the survey spectrum shown in Fig. 2(a), and the high-resolution core level spectrum of the Ti 2p is illustrated in Fig. 2(b), where two main characteristic peaks located at 464.5 and 458.8 eV are ascribed to Ti 2p$_{1/2}$ and Ti 2p$_{3/2}$, respectively. This result reveals the Ti^{4+} oxidation state.[24] Figure 2(c) shows the non-symmetric XPS spectra of O 1s which can be fitted to two peaks, among them the peak at 531.8 eV can be attributed to two cases, i.e., the Ti–OH bond[25] and oxygen in OH$^-$ species absorbed on the surface of $H_2Ti_3O_7$.[23] The peak at 530.1 eV is assigned to the O^{-2} oxidation state, associated with the lattice oxygen Ti–O bond.
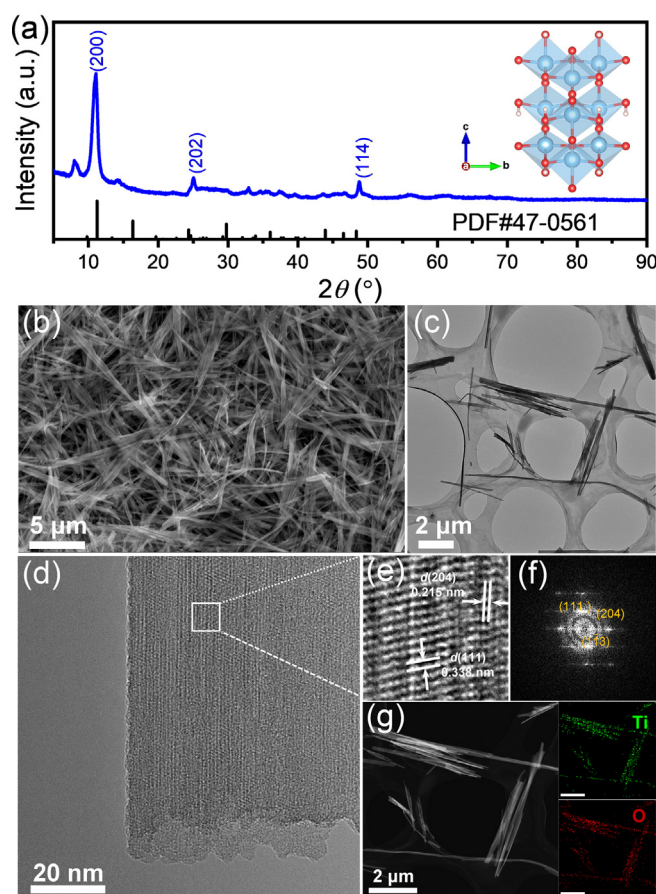

FIG. 1. Structure and morphology characterization of $H_2Ti_3O_7$: (a) XRD pattern, (b) SEM image, (c) TEM image, (d) high-resolution TEM image, the corresponding (e) magnified image and (f) SAED, (g) elemental mapping.
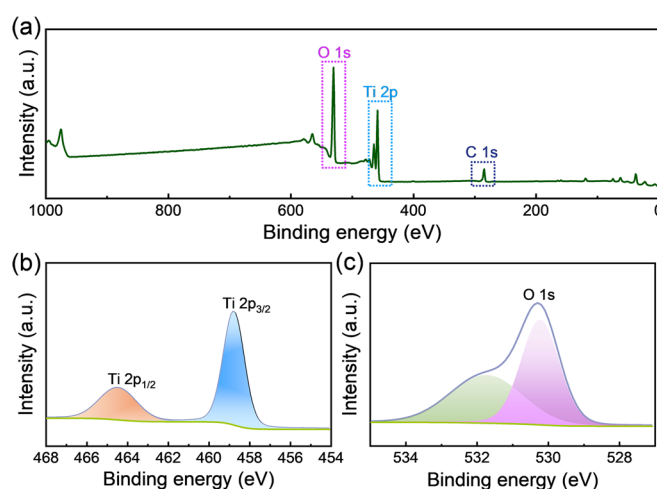

FIG. 2. XPS spectra of $H_2Ti_3O_7$. (a) Survey spectrum, high resolution core level spectra of (b) Ti 2p and (c) O 1s.

To evaluate the CO_2 sonocatalytic reduction performance of the as-synthesized $H_2Ti_3O_7$, CO_2 reduction experiments were carried out under the ultrasonic stimulation as illustrated in Fig. 3. In principle, the prompt recombination of positive and negative charges generated in the sono-reduction reaction severely inhibits the catalytic activities.[26] Since CO_2 reduction is a negative-charge consuming reaction,[27] sacrificial agent sodium sulfide and sodium sulfite are subsequently introduced to neutralize the positive charges in the initial experimental design. In Fig. 3(a), with the addition of positive charge sacrificial agent, the CO_2 is converted into CO, exhibiting a trend of enhanced yield with the increase in the ultrasonic stimulation time. After experiencing 2 h of catalytic time, an average value of 8.3 μmol g^{-1} h^{-1} is achieved. To verify that the CO product originates from sonocatalytic CO_2 conversion process, a controlled experiment of $H_2Ti_3O_7$ catalysts in Ar atmosphere was performed, and there was no detectable CO observed; this indicates that the CO is indeed the product of sonocatalytic CO_2 reduction.

It is reported that ultrasonic vibration itself possesses the sono-chemistry effect,[28] i.e., ultrasonic induced high pressure and temperature directly cause the self-decomposition of CO_2 or other molecules such as water. To rule out the influence of sonochemistry on the CO_2 reduction reaction, a controlled experiment was performed without the addition of $H_2Ti_3O_7$ catalysts. It turns out that the CO yield is negligible, indicating that the sonochemistry effect is weak in the present situation. In addition, a blank experiment was carried out with $H_2Ti_3O_7$ catalysts but without ultrasound stimulation; the result shows no CO yield either. These experiments confirm that the CO yield originates from the ultrasonic vibration enhanced catalytic effect.

To explore the re-usability of $H_2Ti_3O_7$ catalysts, the recycling CO_2 reduction tests were performed under the optimum reaction conditions. As shown in Fig. 3(b), the $H_2Ti_3O_7$ catalysts still possess stable catalytic activity after four consecutive cycles. The structure and morphology results in Figs. S1 and Fig. S2 of the supplementary material show that there is a little difference between fresh and used nanowires. Ultrasonic frequency and power are two factors that directly affect the sonocatalytic activities.[29] Therefore, CO_2 sono-reduction performance of the $H_2Ti_3O_7$ catalysts was quantified on the basis of their CO yield upon the irradiation of various ultrasonic frequencies and power, respectively. Figures 3(c) and 3(d) show that the sonocatalytic CO yield as a function of ultrasonic frequency and power. To specify, when the ultrasonic frequency increases from 28 to 80 kHz, the CO yield rate improves from 0.28 to 8.3 μmol g^{-1} h^{-1}. This enhancement may be attributed to the reinforced mass-transfer effect via boosting ultrasonic frequency.[30] With the improved ultrasonic power, the CO yield also exhibits an enhanced trend; this is due to the fact that the cavitation density is magnified at high ultrasonic power.[31]

To uncover the underlying mechanism of CO_2 sono-reduction, the fundamental process of sonocatalysis was analyzed. Figure 4(a) presents the UV–Vis absorption spectrum of the $H_2Ti_3O_7$ catalysts in the wavelength range of 200–800 nm, where the absorption edge at ∼440 nm can be identified. Based on the equation $(\alpha h\nu)^2 = A(h\nu - E_g)$, where α, $h\nu$, and A are correspondingly the absorption coefficient,
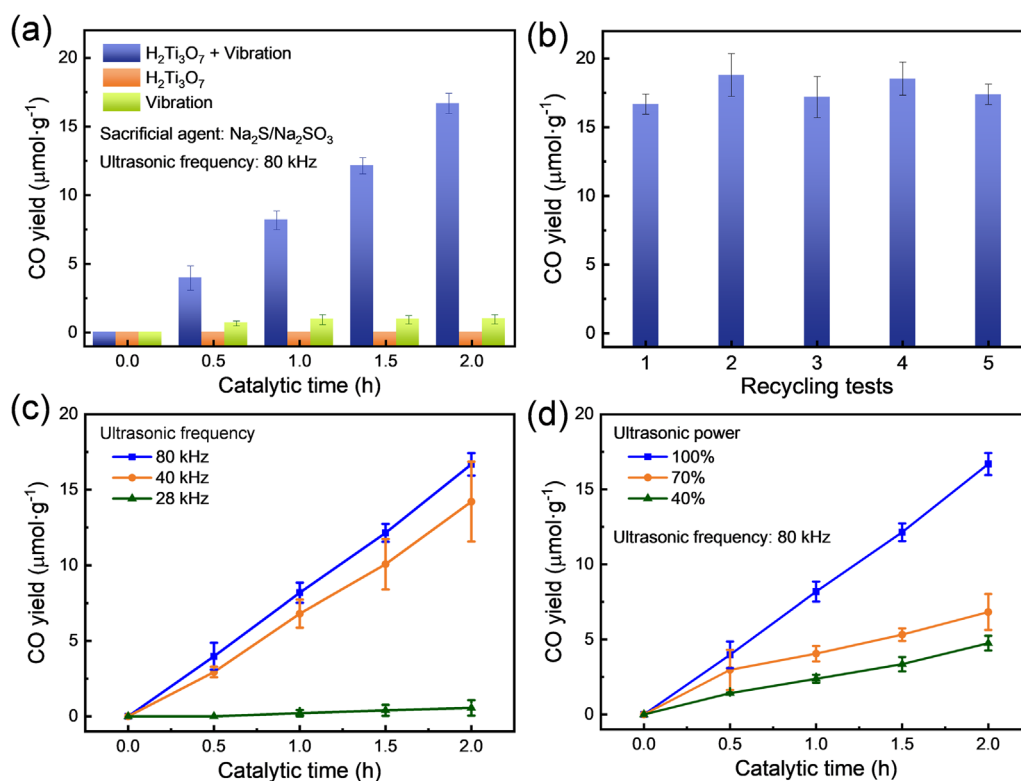
FIG. 3. CO_2 sono-reduction results using $H_2Ti_3O_7$. (a) CO yield through sonocatalytic CO_2 conversion. (b) Recycling CO_2 reduction tests. CO yield under ultrasonic vibration with various (c) vibration frequencies and (d) power. Error bars represent mean ± s.d. obtained from at least two independent experiments.
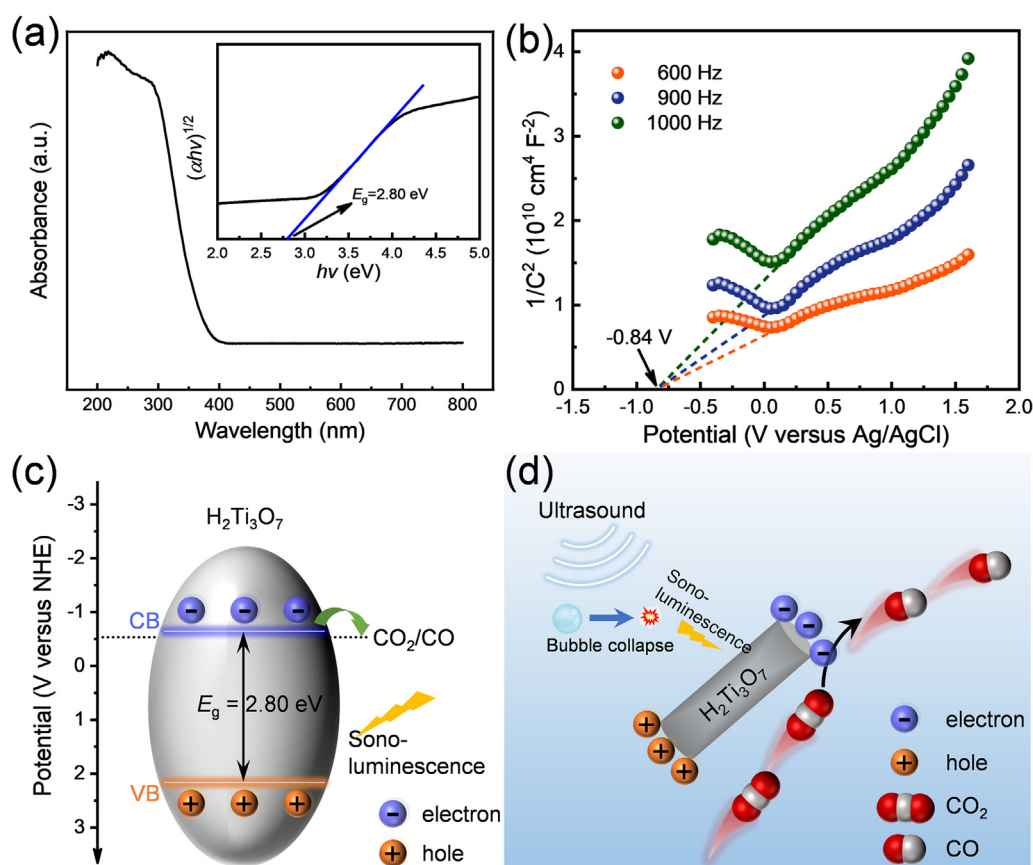
FIG. 4. Mechanism of CO_2 sono-reduction using $H_2Ti_3O_7$. (a) UV–vis absorption spectrum. The inset is a Tauc plot. (b) Mott–Schottky plot, (c) band structure, and (d) schematic of CO_2 sono-reduction.

the incident light energy, and constant,[13] and the inset of Fig. 4(a) illustrates the Tauc plot, from which the optical bandgap E_g is estimated to be ~2.8 eV. The Mott–Schottky plot is further measured to obtain the flatband potential (E_{fb}) of $H_2Ti_3O_7$, as shown in Fig. 4(b), where the positive slope indicates its n-type semiconductor nature. E_{fb} is estimated to be −0.84 V vs Ag/AgCl by extrapolating the linear tangent of abscissa. Through the Nernst equation $E_{NHE} = E_{Ag/AgCl} + 0.197 V$,[32] E_{fb} can be converted into −0.64 V vs NHE. For many n-type semiconductors, E_{fb} is close to the CB potential E_{CB}.[33] Thus, E_{CB} and valence band potential E_{VB} are correspondingly calculated to be −0.64 and 2.16 eV. The band structure of $H_2Ti_3O_7$ is accordingly illustrated in Fig. 4(c), being thermodynamically favorable for CO_2 reduction to CO. A possible mechanism is subsequently proposed. By using ultrasonic vibration as the stimulation to trigger sonocatalysis, a sonoluminescence effect will occur due to the collapse of cavitation bubbles, releasing an emission of light with a wide wavelength range (200–700 nm) and a relatively high intensity.[21] The sonoluminescence-induced light can excite the electrons to CB, leaving holes in CB. The electrons on the suitable CB positions can directly react with CO_2 and convert it to the ultimate product CO as shown in Fig. 4(d).

Piezoelectric materials are generally insulators which may possess proper band structures leading to the sonocatalysis effect under the excitation of ultrasonic vibration, suggesting that the sonocatalysis effect may co-exist in the piezo-electrocatalysis. To exclude the role of the sonocatalysis effect in the piezo-electrocatalysis, two strategies can be considered from the perspective of catalysts and reactions. For piezo-electrocatalysts with identified CB or VB positions, it is suggested to select some reactions whose reduction (oxidation) potentials are much higher (lower) than the CB (VB) position. For reactions which have the clear requirements of reduction/oxidation potentials, it is suggested to look for some piezo-electrocatalysts whose CB or VB are far from meeting the potential requirements in these reactions. In addition, the possible band edge position shift accompanied by the strain, which may enable catalytic reactions by the initially unavailable band structures, should also be taken into consideration.

In summary, the $H_2Ti_3O_7$ nanowire is synthesized via a hydrothermal method and used for sonocatalytic CO_2 reduction. The band structure of $H_2Ti_3O_7$ is determined, in which the CB potential is −0.64 eV, being thermodynamically favorable for CO_2 reduction to CO. Thus, under the ultrasonic vibration with the same experimental process as reported in piezo-electrocatalysis, the non-piezoelectric $H_2Ti_3O_7$ catalyst converts CO_2 into CO with a selectivity of 100%. When the ultrasonic frequencies vary from 28 and 40 to 80 kHz, the CO yield correspondingly reaches 0.28, 7.1, and 8.3 $\mu mol\ g^{-1}\ h^{-1}$ with

the addition of sacrificial agents. In addition, CO yield increases with the increasing ultrasonic power. Note that most piezo-electrocatalysts also possess suitable band structures and may have the sonocatalysis effect, which may be one of the reasons for the disputes in piezo-electrocatalytic mechanisms. This work suggests taking account of and excluding the sonocatalysis effect via exploring the mechanism of piezo-electrocatalysis in the future.

See the supplementary material for details regarding the material preparation and characterization, electrochemical measurements, sonocatalytic activity tests, and for the supporting figures of XRD, SEM, TEM, and XPS.

AUTHOR DECLARATIONS
Conflict of Interest

The authors have no conflicts to disclose.

Author Contributions

Jiangping Ma: Investigation (equal); Visualization (equal); Writing – original draft (equal). **Xin Xiong:** Visualization (equal). **Chaogang Ban:** Visualization (equal). **Kaiwen Wang:** Visualization (equal). **Jiyan Dai:** Funding acquisition (equal); Writing – review & editing (equal). **Xiaoyuan Zhou:** Conceptualization (equal); Funding acquisition (equal); Writing – review & editing (equal).

DATA AVAILABILITY

The data that support the findings of this study are available within the article and its supplementary material.

REFERENCES

[1] W. Ma, S. Xie, T. Liu, Q. Fan, J. Ye, F. Sun, Z. Jiang, Q. Zhang, J. Cheng, and Y. Wang, Nat. Catal. **3**(6), 478 (2020).

[2] J. Timoshenko, A. Bergmann, C. Rettenmaier, A. Herzog, R. M. Arán-Ais, H. S. Jeon, F. T. Haase, U. Hejral, P. Grosse, and S. Kühl, Nat. Catal. **5**(4), 259 (2022); C.-T. Dinh, T. Burdyny, M. G. Kibria, A. Seifitokaldani, C. M. Gabardo, F. P. García de Arquer, A. Kiani, J. P. Edwards, P. De Luna, and O. S. Bushuyev, Science **360**(6390), 783 (2018); R. G. Mariano, K. McKelvey, H. S. White, and M. W. Kanan, *ibid.* **358**(6367), 1187 (2017).

[3] J. Meng, Y. Duan, S. Jing, J. Ma, K. Wang, K. Zhou, C. Ban, Y. Wang, B. Hu, and D. Yu, Nano Energy **92**, 106671 (2022); Y. Feng, Y. Wang, K. Wang, J. Ma, Y. Duan, J. Liu, X. Lu, B. Zhang, G. Wang, and X. Zhou, Rare Met. **41**(2), 385 (2022); C. Ban, Y. Duan, Y. Wang, J. Ma, K. Wang, J. Meng, X. Liu, C. Wang, X. Han, and G. Cao, Nano-Micro Lett. **14**(1), 74 (2022); Y. Feng, Y. Wang, K. Wang, C. Ban, Y. Duan, J. Meng, X. Liu, J. Ma, J. Dai, and D. Yu, Nano Energy **103**, 107853 (2022).

[4] B. M. Tackett, E. Gomez, and J. G. Chen, Nat. Catal. **2**(5), 381 (2019).

[5] J. Curie and P. Curie, Bull. Mineral. **3**(4), 90 (1880), available at https://www.persee.fr/doc/bulmi_0150-9640_1880_num_3_4_1564.

[6] R. Ryndzionek, M. Michna, M. Ronkowski, and J.-F. Rouchon, IEEE/ASME Trans. Mechatron. **23**(5), 2178 (2018).

[7] Y. Qin, X. Wang, and Z. L. Wang, Nature **451**(7180), 809 (2008); Z. L. Wang and J. Song, Science **312**(5771), 242 (2006).

[8] D. Y. Park, D. J. Joe, D. H. Kim, H. Park, J. H. Han, C. K. Jeong, H. Park, J. G. Park, B. Joung, and K. J. Lee, Adv. Mater. **29**(37), 1702308 (2017); Y. Saito, H. Takao, T. Tani, T. Nonoyama, K. Takatori, T. Homma, T. Nagaya, and M. Nakamura, Nature **432**(7013), 84 (2004).

[9] E. Tekin, P. J. Smith, and U. S. Schubert, Soft Matter **4**(4), 703 (2008); R. E. Saunders, J. E. Gough, and B. Derby, Biomaterials **29**(2), 193 (2008).

[10] Y. Qiu, J. V. Gigliotti, M. Wallace, F. Griggio, C. E. Demore, S. Cochran, and S. Trolier-McKinstry, Sensors **15**(4), 8020 (2015).

[11] K.-S. Hong, H. Xu, H. Konishi, and X. Li, J. Phys. Chem. Lett. **1**(6), 997 (2010).

[12] L. Chen, Y. Jia, J. Zhao, J. Ma, Z. Wu, G. Yuan, and X. Cui, J. Colloid Interface Sci. **586**, 758 (2021); Y. Hong, J. Ma, Z. Wu, J. Ying, H. You, and Y. Jia, Acta Phys. Sin. **67**(10), 107702 (2018).

[13] J. Ma, J. Ren, Y. Jia, Z. Wu, L. Chen, N. O. Haugen, H. Huang, and Y. Liu, Nano Energy **62**, 376 (2019).

[14] K. Kubota, Y. Pang, A. Miura, and H. Ito, Science **366**(6472), 1500 (2019).

[15] Y. Wang, X. Wen, Y. Jia, M. Huang, F. Wang, X. Zhang, Y. Bai, G. Yuan, and Y. Wang, Nat. Commun. **11**(1), 1328 (2020).

[16] P. Zhu, Y. Chen, and J. Shi, Adv. Mater. **32**(29), 2001976 (2020).

[17] Y. Wang, Y. Xu, S. Dong, P. Wang, W. Chen, Z. Lu, D. Ye, B. Pan, D. Wu, and C. D. Vecitis, Nat. Commun. **12**(1), 3508 (2021).

[18] J. Ma, S. Jing, Y. Wang, X. Liu, L. Y. Gan, C. Wang, J. Y. Dai, X. Han, and X. Zhou, Adv. Energy Mater. **12**, 2200253 (2022).

[19] S. Tu, Y. Guo, Y. Zhang, C. Hu, T. Zhang, T. Ma, and H. Huang, Adv. Funct. Mater. **30**(48), 2005158 (2020); W. Qian, W. Yang, Y. Zhang, C. R. Bowen, and Y. Yang, Nano-Micro Lett. **12**(1), 1 (2020); S. Li, Z. Zhao, Z. Zhang, X. Li, and J. Zhang, ACS Appl. Nano Mater. **3**(2), 1063 (2020).

[20] K. Wang, C. Han, J. Li, J. Qiu, J. Sunarso, and S. Liu, Angew. Chem., Int. Ed. **134**(6), e202110429 (2022); F. Bößl and I. Tudela, Curr. Opin. Green Sustainable Chem. **32**, 100537 (2021).

[21] P. Qiu, B. Park, J. Choi, B. Thokchom, A. B. Pandit, and J. Khim, Ultrason. Sonochem. **45**, 29 (2018).

[22] C. Wang, T. Ma, Y. Zhang, and H. Huang, Adv. Funct. Mater. **32**(5), 2108350 (2022).

[23] M. Du, G. Zeng, J. Huang, D. Sun, Q. Li, G. Wang, and X. Li, ACS Sustainable Chem. Eng. **7**(10), 9717 (2019).

[24] A. Sarkar, K. Karmakar, A. K. Singh, K. Mandal, and G. G. Khan, Phys. Chem. Chem. Phys. **18**(38), 26900 (2016).

[25] Y. Xu, J. L. L. Yao, L. L. P. Yang, and N. Huang, Surf. Coat. Technol. **261**, 436 (2015).

[26] N. Merabet and K. Kerboua, Int. J. Hydrogen Energy **47**(41), 17879 (2022).

[27] A. Goyal, G. Marcandalli, V. A. Mints, and M. T. Koper, J. Am. Chem. Soc. **142**(9), 4154 (2020).

[28] H. Harada, Ultrason. Sonochem. **5**(2), 73 (1998).

[29] E. C. Gaudino, G. Cravotto, M. Manzoli, and S. Tabasso, Chem. Soc. Rev. **50**(3), 1785 (2021).

[30] N. M. Navarro, T. Chave, P. Pochon, I. Bisel, and S. I. Nikitenko, J. Phys. Chem. B **115**(9), 2024 (2011).

[31] V. Sivakumar and R. Mohan, Appl. Phys. A **128**(1), 27 (2022).

[32] C. Wan, L. Zhou, L. Sun, L. Xu, D. Cheng, F. Chen, X. Zhan, and Y. Yang, Chem. Eng. J. **396**, 125229 (2020).

[33] J. Li, H. Huang, W. Xue, K. Sun, X. Song, C. Wu, L. Nie, Y. Li, C. Liu, and Y. Pan, Nat. Catal. **4**(8), 719 (2021).